Cavity Catalysis by Co-operative Vibrational Strong Coupling of Reactant and Solvent Molecules

Jyoti Lather[a], Pooja Bhatt[a], Anoop Thomas[b], Thomas W. Ebbesen[b]*, Jino George[a]*

[a]*Department of Chemical Sciences, Indian Institute of Science Education and Research (IISER) Mohali, Punjab-140306, India.*
[b]*University of Strasbourg, CNRS, ISIS & icFRC, 8 allée G. Monge, 67000 Strasbourg, France.*

ABSTRACT: *para*-nitrophenyl acetate (PNPA) hydrolysis is studied under vibrational strong coupling (VSC) in a Fabry-Perot micro-fluidic cavity. By tuning the cavity resonance to the C=O vibrational stretching mode of both the reactant and solvent molecules, it is found that the reaction is accelerated by an order of magnitude. It is shown that this cavity catalysis involves a co-operative strong coupling effect between the solvent and the reactant molecules. The reaction rate follows an exponential relation with respect to the solvent coupling strength. The combination of co-operative effects and cavity catalysis confirms the potential of VSC as a new frontier in chemistry.

Over the last century, synthetic organic chemistry has undergone spectacular development by mastering the ways of controlling reactions.[1,2] Nevertheless, modifying the energy landscape of an intrinsic reaction co-ordinate remains a challenging task. The concept of coherent chemistry was introduced to address this issue of targeting a chemical bond with intense field thereby pushing the bond oscillations to overcome the transition state (TS) energy.[3] One of the challenging aspects of coherent chemistry is that the applied energy will be redistributed into 3N-6 degrees of freedom and hence the process is less efficient.[4,5]

Strong light-matter coupling offers a unique way of controlling internal reaction coordinates by coupling molecular transitions to the vacuum field (zero-point energy) of a cavity mode.[6,7] VSC was introduced to couple selectively a vibrational mode.[8,9] VSC is most easily achieved in the liquid state in a microfluidic Fabry-Perot (FP) cavity.[10] Thomas *et al*., observed the modification of the rate of a C-Si bond breaking process and more interestingly changes to the branching ratio of products by selective VSC of silane derivatives.[11a, b] Recently, Hiura *et al* reported the possibility of cavity catalysis by vibrational ultra-strong coupling of water molecules involved in hydrolysis reactions.[12] In both the cases, reactants were directly coupled to the cavity modes and the reaction rates could be controlled by moving the physical distance between the mirrors of an FP cavity, i.e. by tuning the coupling to a given vibrational mode. Recent theoretical studies confirm that potential energy surfaces and reactivity can be modified by coupling to the vacuum field.[13-16]

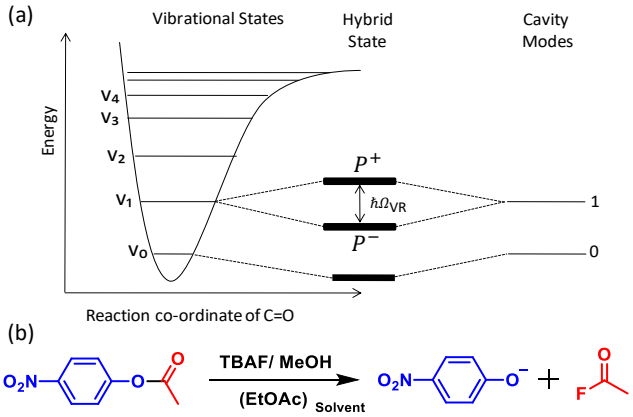

Figure 1. (a) Schematic representation of vibro-polaritonic states formed from a molecular vibrational state and a FP cavity mode; (b) the hydrolysis of PNPA in ethyl acetate (EtOAc).

VSC condition can be achieved by injecting a molecular liquid into a FP cavity in which the vibrational band interact with the cavity mode (Figure 1a) to generate two new eigen states, called vibro-polaritonic states (P+ and P-). The interaction energy (Rabi energy; $\hbar\Omega_{\mathrm{VR}}$) is proportional to the oscillator strength (f) and the electric field (E) of the electromagnetic mode of the cavity:

$$\hbar\Omega_{\mathrm{VR}} \propto 2f \cdot E \times \sqrt{n_{\mathrm{ph}}+1}; E = \sqrt{\frac{\hbar\omega}{2\varepsilon_0 V}} \qquad (1)$$

where ε_0 is the vacuum permittivity, ω is the vibrational frequency, V is the mode volume of the cavity and n_{ph} the number of photons involved in the coupling process. When the latter goes to zero, a residual Rabi splitting energy remains even in the dark due to the coupling to the zero-point energy of the cavity. Importantly, $\hbar\Omega_{\mathrm{VR}}$ is proportional to $\sqrt{N/V} \sim \sqrt{C}$ where N is the number and C the concentration of the coupled molecules interacting strongly with the cavity mode. [6-8]

In this communication, we report the hydrolysis of PNPA catalyzed by VSC under co-operative strong coupling effect between the solvent and the reactant molecules. In other words, when the vibrational frequency of reactant molecules exactly matches with cavity mode, which is in the envelope of solvent vibro-polaritonic reservoir, it increases the reaction rate more than one order of magnitude at room temperature.

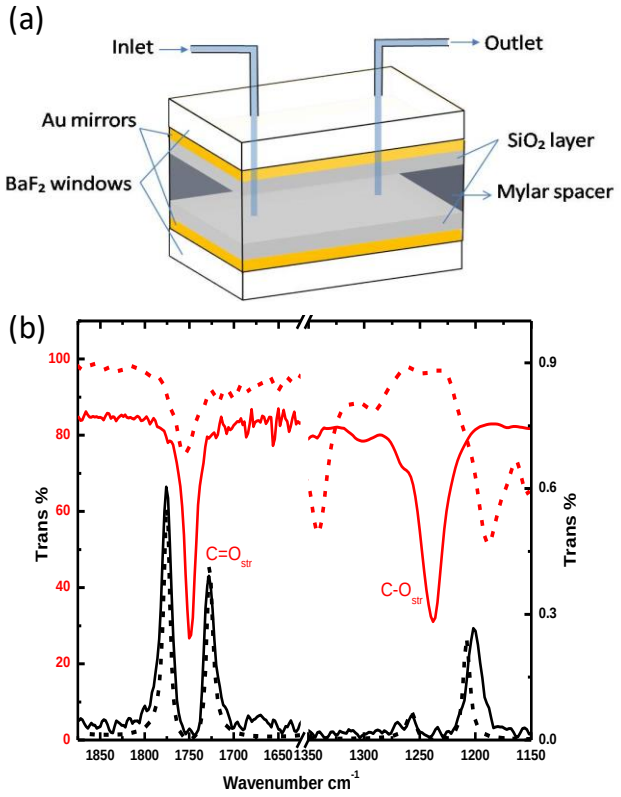

Figure 2. (a) Schematic representation of a flow cell FP cavity. (b) IR transmission spectra of 10 % EtOAc (red trace) and ATR spectrum of neat PNPA (dotted red trace). Vibro-polaritonic states P+ and P- formed by coupling to the 10th and 7th cavity modes to carbonyl and acyl bands of EtOAc respectively (black trace; pathlength is approx. 18 μm); dotted black trace represent the corresponding TMM simulation.

The FP cavities used in the present experiments were prepared with Au mirrors sputtered on to IR transparent BaF_2 windows, following a reported procedure.[10] The spacing between the mirrors used for the current study is approximately 18 μm (Figure 2a, b). Such FP cavities can hold up to 3 μL volume of reacting solution. The non-cavity experiments were carried out in a microfluidic cell made of bare BaF_2 windows. See Supporting Information for further details. PNPA hydrolysis[17] in this study was carried out under mild basic conditions provided by tetrabutylammonium fluoride (TBAF), as schematically shown in Figure 1b. EtOAc was chosen as the solvent because its carbonyl stretching transition overlaps with that of the reactant PNPA (Figure 2b; red traces). Both PNPA and TBAF solutions were prepared separately, mixed outside and injected into the FP cavity.

Strong coupling of the C=O stretching mode of neat EtOAc to the 10th mode of the FP cavity gives a Rabi splitting of 155 cm^{-1}, which is equivalent to 4.4 % change in the actual transition energy with P+ and P- are at 1840 cm^{-1} and 1685 cm^{-1}, respectively (Figure 2b and Figure S2). In the reactive mixture, only EtOAc (99.9 w % compared to PNPA) gets coupled to the cavity mode effectively. Now the question is whether VSC of EtOAc will influence the reactivity of PNPA in such conditions?

The major product of the PNPA hydrolysis is the para-nitro phenoxide (PNP-) having an intense absorption peak at 407 nm. Since the transparency region of BaF_2 windows extends well in to the UV (c.a. 300 nm), the progress of the reaction can be easily monitored by following the temporal rise of PNP- absorption peak as shown

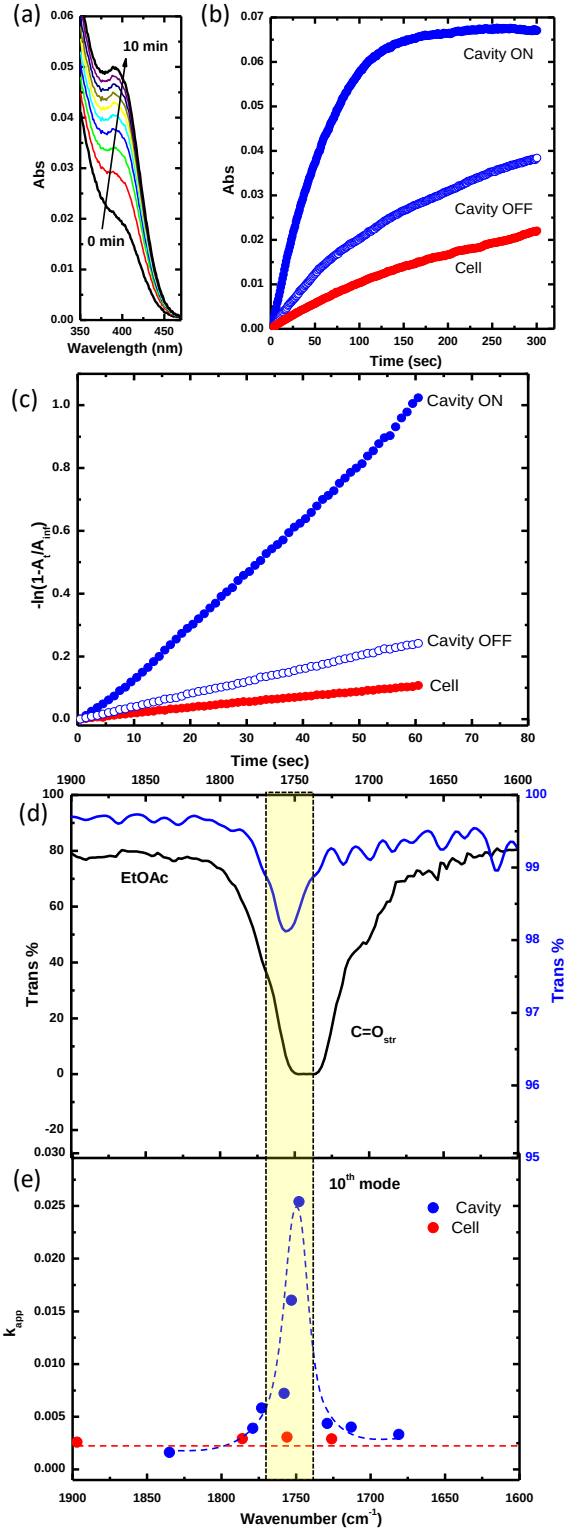

Figure 3. (a) Absorption spectra in a cell (non-cavity) shows the temporal evolution of PNP^- during the ester hydrolysis. (b) Kinetic traces measured at 407 nm and (c) the corresponding log-plot of cavity ON resonance (blue circle; 1753 cm^{-1}), cavity OFF resonance (blue hollow circle; 1713 cm^{-1}) and cell (red circle). (d) Carbonyl stretching mode of 0.1 M PNPA (grey trace) and 100 % EtOAc (black trace). (e) k_{app} verses tuning the cavity mode frequency (blue circle) indicate the rate enhancement only happens in the C=O stretch region at ON resonance and the corresponding k_{app} at four different pathlength in the cell (non-cavity; red circle). *The dashed curves are guides to eye.*

in Figure 3a. In other words, while the FP cavity is set to couple the C=O vibrational band in the IR, the influence of strong coupling on the reaction rate is being monitored in the UV-Vis region. This condition help to avoid complications such as filter effects and other issues related to FP cavity configuration. By having a tenfold excess of PNPA as compared to TBAF (0.1 M vs 0.01M), a pseudo-first order kinetics was observed. Apparent rates (k_{app}) were determined by linear regression method (Figure 3b, c).[17] In the normal cell (non-cavity), the apparent rate constant k_{app}^{cell} is in the order of 0.2 x 10^{-2} s^{-1} (Figure 3b, c). To prepare an ON-resonance cavity, the empty cavity is tuned slowly to the desired pathlength and is kept undisturbed for 30 minutes (for details see Supporting Information). Subsequently, the reaction mixture is injected into the cavity and the kinetic traces are recorded. Under ON-resonance condition, in other words when the cavity is tuned to C=O stretching frequency of the EtOAc, the k_{app}^{cav} increased by more than one order of magnitude (2.5 x 10^{-2} s^{-1}) compared to the non-cavity as shown in Figure 3b, and c. k_{app}^{cav} levels off to normal values (k_{app}^{cell}) when the cavity is detuned from the C=O mode (the OFF-resonance measurements) as shown in Figure 3e. Please note that the cell (non-cavity) and the cavity conditions are exactly the same, except the presence of Au mirrors in cavity, and k_{app}^{cell} is unaffected by small variation in the spacer thickness (red circle in the Figure 3e). Interestingly, k_{app}^{cav} follows the vibration envelope of C=O stretching mode of solvent molecules that coupled to the 10^{th} cavity mode (Figure 3d and e). The increase in the k_{app}^{cav} specifically at the carbonyl stretching mode roughly follow its full width-half maximum (FWHM; 25 cm^{-1}). TBAF/MeOH mixture provides methoxide ions, attacking the electron deficient C=O carbon atom which is considered as the rate determining step.[17b, c] This is a clear indication that the VSC of EtOAc can co-operatively transfer the coupling strength to the C=O stretching mode of PNPA that can influence its internal reaction coordinate so as to affect its bond dissociation energy.

Another interesting aspect of the study is to look into the reaction rate variation (PNPA concentration was fixed at 0.1 M) with respect to co-operative coupling strength of the solvent molecules. To our surprise, an exponential rise in the reaction rate is observed upon further increasing the concentration of EtOAc under strong coupling condition (Figure 4). We have chosen anisole as a co-solvent (polarity difference is 0.03) with EtOAc to avoid rate change due to solvent co-ordination on the transition state and negligible changes are indeed observed in the cell medium (Figure S3). We propose two possibilities for decreasing the bond dissociation energy. First, solvent molecules are involved here in the charge stabilization of the transition state, which could be further stabilized under VSC conditions. Secondly, the VSC of the C=O stretching mode of the solvent can be transferred to solute PNPA through solute-solvent interactions, thereby modifying the reaction co-ordinate. The later has been investigated theoretically and confirmed to be possible depending on the strength of the solute-solvent interactions.[19]

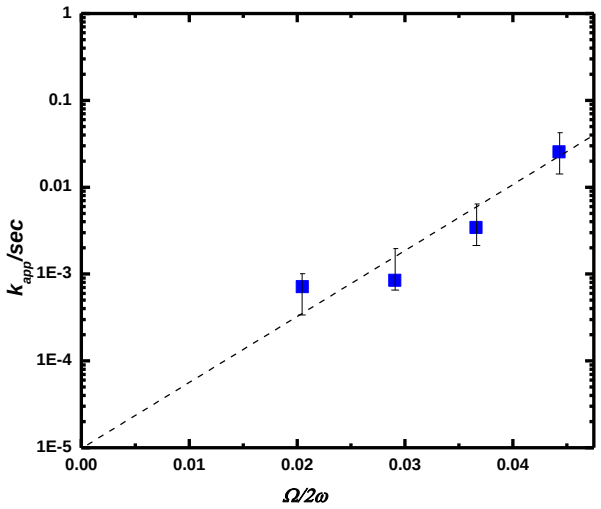

Figure 4. Semi-logarithmic plot showing apparent rates by varying co-operative coupling strength of the solvent molecules at ON resonance condition.

In conclusion, we have shown that a chemical reaction can be catalyzed by coupling solvent molecules to vacuum field without direct involvement of the solvent in the reaction. This is specifically achieved through a co-operative interaction between the solute and the strongly coupled solvent. Detuning experiments clearly indicate the feasibility of controlling the chemical energy landscape by modifying the internal reaction coordinate. Concentration dependent studies points to the fact that co-operativity in strong coupling influence the reaction rate through an exponential relation and this can also be related to a change in the anharmonicity factor of the Morse potential curve.[12,18] All these finding should have large impact on controlling chemical reactivity through VSC. More experiments are underway in order to understand the actual mechanism of such modifications under VSC of solvents.

Supporting Information

Experimental Methods:

para-nitrophenyl acetate (PNPA) and tetrabutylammonium fluoride (TBAF) were purchased from Sigma-Aldrich. HPLC grade ethyl acetate, anisole and methanol are purchased (Merck Life Science) and used as such for the experiments. Ester hydrolysis of PNPA in mild basic condition of TBAF was carried out by mixing 0.1M PNPA (18mg PNPA in 1mL ethyl acetate) and 0.1M TBAF (31.5mg in 1mL methanol). Fresh solutions were used for each experiment. The reactant (0.1M PNPA) and the reagent (0.1M TBAF) are mixed in 9: 1 ratio, in a 4 mL glass vial and 300 µL of this reaction mixture was injected immediately into the FP cavity with a standard disposable syringe. Final concentrations of PNPA and TBAF are 0.1M and 0.01M respectively. The rate of the reaction is followed by observing the absorbance at 407 nm and kinetic data are plotted by observing the system up to 300 seconds.

TBAF normally dissolves in polar protic solvent and the fluoride ions are stabilized by intermolecular H- bonding with solvent molecules. In methanol, TBAF-fluoride can abstract a proton which generate methoxide species which attack the electron deficient carbonyl carbon atom. This nucleophilic attack of methoxide ion on the electron deficient carbonyl carbon generate a tetrahedral intermediate state.[17] *para*-nitrophenyl (PNP) group is more electron withdrawing, resulted in reshuffling of electron density leads to the formation of *para*-nitrophenoxide ions. Please note the rate determining step is the formation of the tetrahedral intermediate which involve the attack of the nucleophile on the carbonyl group.

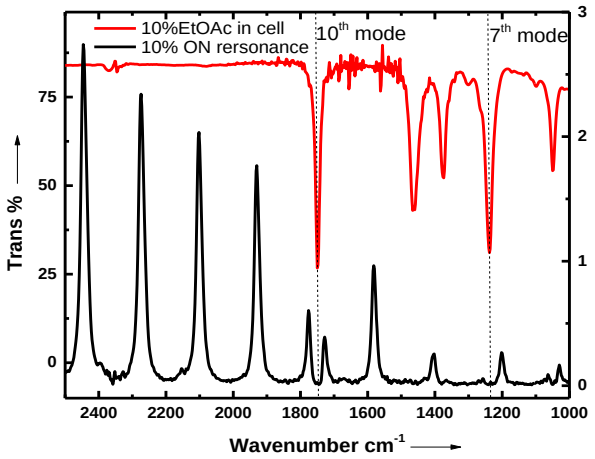

Figure S1: IR transmission spectra of PNPA in 10% EtOAc (red trace) and the corresponding P+ and P- formed by coupling to the 10th and 7th cavity mode (black trace).

Demountable flow cell with BaF_2 windows was purchased from Specac Ltd. UK and used for the studies. Mylar spacers with 18 µm thickness was used for the cell as well as the cavity experiments. 4 mm thick BaF_2 windows was coated with 10 nm Au film by thermal evaporation method and 100 nm of SiO_2 passivating layer is deposited by RF sputtering onto the Au film. IR spectra were recorded by Perkin-Elmer FT-IR spectrophotometer (Spectrum 1). Cavity modes are tuned precisely by tightening or loosening the four precision screws on different corners of the flow cell. Free spectral range (FSR) is measured in every case by taking the average of 6 cavity modes of an empty cavity and by back calculation we achieve ON resonance situation from the beginning of the injection of the reaction mixture (Figure S1; Table 1). Calculation of the FSR can be done by using the formula; $k(cm^{-1}) = \frac{10000}{2nL}$, where n is refractive index (RI) of medium and L is the length between the mirrors (µm). RI of the solution was estimated a priori for achieving ON resonance situation and the actual FSR is measured to cross-check after the completion of the reaction, assuming that the product formed will not change the RI of the medium during the course of the reaction. Please note that in this regard, the reactant concentration is 1, 000 times lower than the solvent medium. After setting the empty cavity FSR, system is kept at rest for 30 minutes. Both the reactant and the reagent are maintained at 30° C in a water bath for equilibration and the reaction mixture was injected into the cavity followed by observing the kinetic traces at 407 nm in a UV-Vis spectrophotometer (Carry 5000).

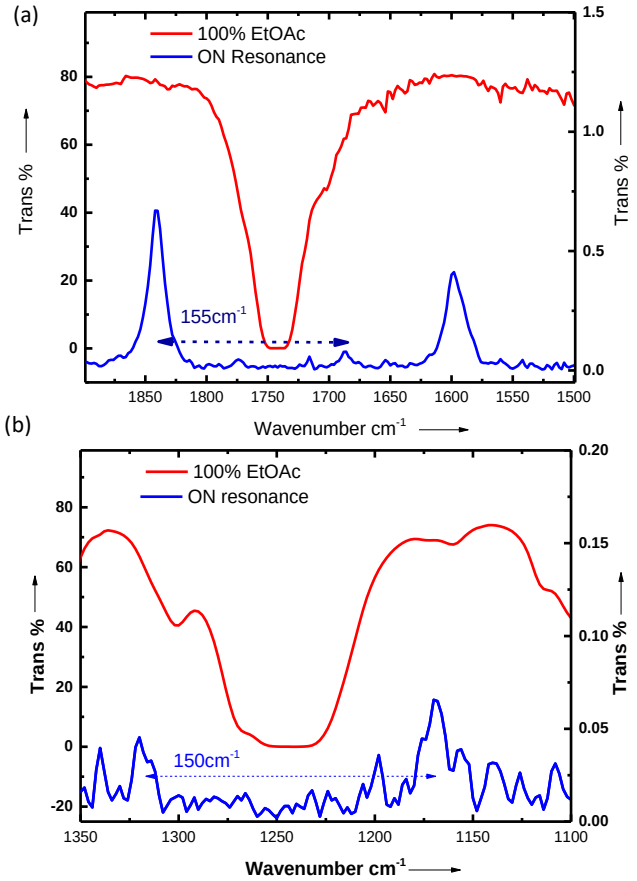

Figure S2: IR spectra of pure EtOAc (red trace) and the corresponding P+ and P- formed by coupling the (a) 10th mode of the cavity to carbonyl and (b) 7th mode of the cavity to acyl bands (blue traces).

IR spectra of EtOAc exhibit carbonyl C=O and acyl C-O stretching mode at 1750 cm^{-1} and1238 cm^{-1}, respectively. Coupling the 10th mode of the cavity to the carbonyl band of EtOAc resulted in a Rabi Splitting energy of 155 cm^{-1} with P+ and P- at 1840 cm^{-1} and 1685 cm^{-1} respectively (Figure S2). The 7th mode of the cavity can be resonantly coupled to acyl vibrational mode having Rabi energy of 150 cm^{-1} with P+ and P- at 1320 cm^{-1} and 1170 cm^{-1}, respectively. The number of molecules calculated from the concentration and volume occupied (3µL) is roughly 10^{15} for PNPA and 10^{18} for ethyl acetate molecules.

Next, we compared the change in the solvent mixture with respect to the reaction rate. Here, the cell was maintained at the same path-length and kinetics was measured by varying the concentration of EtOAc from 25% to 100% in a step of 25%. Anisole was taken as the mixing solvent due to similar polarity as that of EtOAc. The reaction rate for varying concentration of EtOAc is plotted in

Figure S3. It should be noted that the rate increase is negligible compared to the VSC condition as mentioned in the Figure 4.

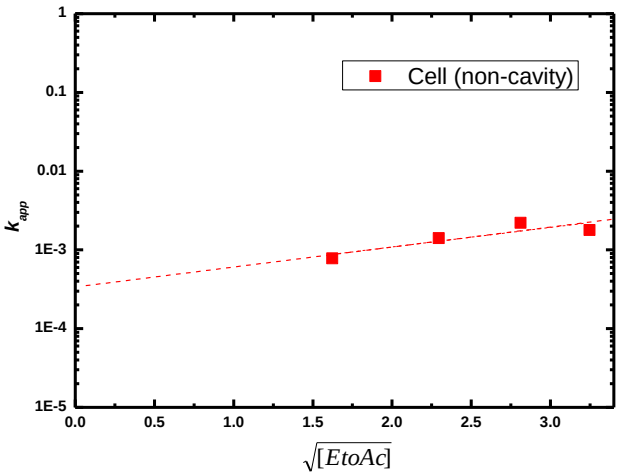

Figure S3: Semi-logarithmic plot of apparent rate verses square root of concentration of EtOAc.

Table S1: FSR of the empty cavity and reacting medium inside the QED reactor and the corresponding rate as plotted in Figure 3e.

s.no.	Empty cavity free spectral range	FSR after injecting reaction mixture	K(reaction rate)s^{-1}
1	240.46	174.9	2.54 X 10^{-2}
2	239.91	175.5	0.72 X 10^{-2}
3	240.29	175.3	1.61 X 10^{-2}
4	236.96	172.9	0.44 X 10^{-2}
5	233.9	171.3	0.40 X 10^{-2}
6	245.13	177.9	0.33 X 10^{-2}
7	230.5	168.2	0.33 X 10^{-2}
8	251.3	183.5	0.16 X 10^{-2}

Transfer Matrix Method (TMM) simulation:

Transfer Matrix Method (TMM) simulation predict approximately the cavity modes, by solving Maxwell equation for multiple layers having different refractive indices during the light propagation. Here, we constructed a multilayer index medium with pure Au mirrors (thickness; approx. 10 nm), dielectric SiO_2 (100 nm; refractive index data was taken from https://refractiveindex.info). The mirror spacing are tuned to achieve strong coupling condition with carbonyl stretching mode. 10^{th} mode of the cavity is coupled to the C=O stretch and the bulk RI was taken approx. as 1.37.

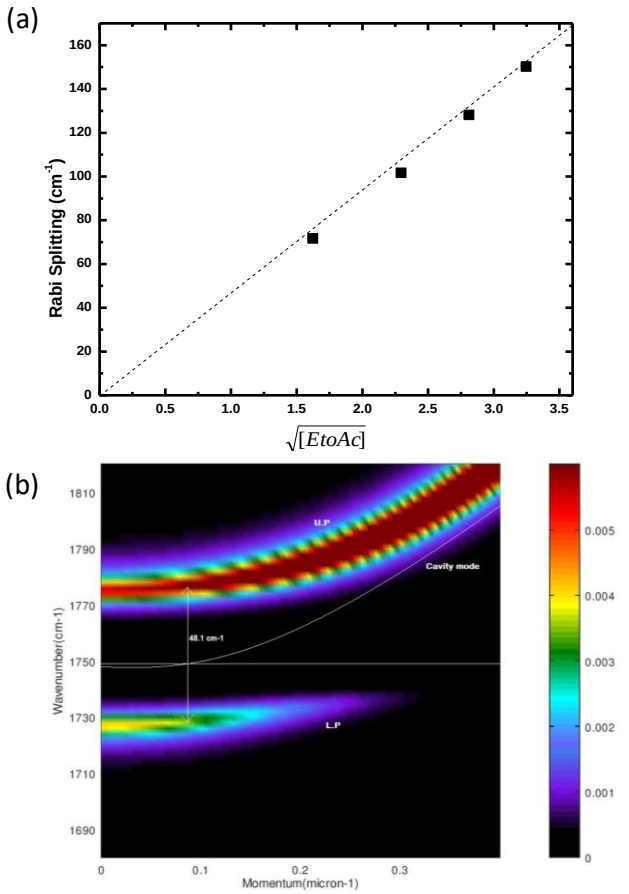

Figure S4: (a) Rabi splitting verses square root of concentration of EtOAc; C=O stretching band is at ω_0=1750 cm^{-1} and (b) the dispersion curve for carbonyl VSC for 10% EtOAc.

AUTHOR INFORMATION

Corresponding Authors

ebbesen@unistra.fr
jgeorge@iisermohali.ac.in

ACKNOWLEDGMENT

J.G. would like to thank IISER Mohali for funding and Department of Chemical Sciences, IISER Mohali for using the facilities; DST-SERB, Core Research Grant (EMR/2017/003455) is also acknowledged. J. L. and P. B. thank IISER Mohali for research funding.

REFERENCES

(1) (a) Wender, P. A. *Chem. Rev.* **1996**, *96*, 1. (b) Carreira, E. M. *Chem. Rev.* **2015**, *115*, 8945.
(2) Balzani, V.; Ceroni, P.; Juris, A. *Molecular organic Photochemistry* Chapter 7 (p. 169-189), *Photochemistry and Photophysics-Concept, Research and Application* Wiley-VCH, Verlay GmbH and Co-KGaA, **2014**.
(3) Frei, H.; Pimentel, G. C. *J. Chem. Phys.* **1983**, *78*, 3698.
(4) Zewail, A. H. *J. Phys. Chem. A* **2000**, *104*, 5660.
(5) Baskin, J. S.; Zewail, A. H. *J. Chem. Edu.* **2001**, *78*, 737.
(6) Ebbesen, T. W. *Acc. Chem. Res.* **2016**, *49*, 2403–2412.
(7) Hutchison, J. A.; Schwartz, T.; Genet, C.; Devaux, E.; Ebbesen, T. W. *Angew. Chem. Int. Ed.* **2012**, *51*, 1592.

(8) Shalabney, A.; George, J.; Hutchison, J.; Pupillo, G.; Genet, C.; Ebbesen, T. W. *Nat. Commun.* **2015**, *6*, 5981.
(9) Long, J. P.; Simpkins, B. S. *ACS Photonics* **2015**, *2*, 130.
(10) George, J.; Shalabney, A.; Hutchison, J. A.; Genet, C.; Ebbesen, T. W. *J. Phys. Chem. Lett.* **2015**, *6*, 1027.
(11) (a) Thomas, A.; George, J.; Shalabney, A.; Dryzhakov, M.; Varma, S. J.; Moran, J.; Chervy, T.; Zhong, X.; Devaux, E.; Genet, C.; Hutchison, J. A.; Ebbesen, T. W. *Angew. Chem. Int. Ed.* **2016**, *55*, 11462; (b) Thomas, A., Lethuillier-Karl, L.; Nagarajan, K.; Vergauwe, R. M. A.; George, J.; Chervy, T.; Shalabney, A.; Devaux, E.; Genet, C.; Moran, J.; Ebbesen, T. W. https://doi.org/10.26434/chemrxiv.7160789.v1.
(12) Hiura, H.; Shalabney, A.; George, J. https://doi.org/10.26434/chemrxiv.7234721.v3
(13) (a) Flick, J.; Ruggenthaler, M.; Appel, H.; Rubio, A. *Proc. Natl. Acad. Sci. USA.* **2017**, *114*, 3026. (b) Ruggenthaler, M.; Tancogne-Dejean, N.; Flick, J.; Appel, H.; Rubio, A. *Nat. Rev. Chem.* **2018**, *2*, 0118.
(14) Ribeiro, R. F.; Martinez-Martinez, L. A.; Du, M.; Campos-Gonzalez-Angulo, J.; Yuen-Zhou, *J. Chem. Sci.* **2018**, **9**, 6325-6339.
(15) (a) Herrera, F.; Spano, F. C. *Phys. Rev. Lett.* **2016**, *116*, 238301. (b) Herrera, F.; Spano, F. C. *ACS Photonics* **2018**, *5*, 65.
(16) (a) Galego, J.; Garcia-Vidal, F. J.; Feist, J. *Nat. Commun.* **2016**, *7*, 13841. (b) Galego, J.; Garcia-Vidal, F. J.; Feist, J. *Phys. Rev. Lett.* **2017**, *119*, 136001; (c) Galego, J.; Climent, C.; Garcia-Vidal, F. J.; Feist, J. arXiv:1807.10846.
(17) (a) Park, J. H.; Meriwether, B. P.; Clodfelder, P.; Cunningham, L. W. *J. Bio. Chem.* **1961**, *236*, 136; (b) Clark, J. H. *Chem. Rev.* **1980**, *80*, 429; (c) Jencks, W. P.; Gilchrist, M. *J. Am. Chem. Soc.* **1968**, *90*, 2622.
(18) (a) Teller, E. *J. Phys. Chem.* **1937**, *41*, 109; (b) Hanggi, P.; Talkner, P.; Borkovec, M. *Rev. Mod. Phys.* **1990**, *62*, 251.
(19) Hagenmüller, D.; Schütz, S.; Schachenmayer, J.; Ebbesen, T.W.; Genes, C.; Pupillo, G. ArXiv (**2018**).